Int J Clin Exp Med 2017;10(12):16121-16132
www.ijcem.com /ISSN:1940-5901/IJCEM0059248

Original Article

Relationship between anterior cerebral falx and craniofacial midline: significance in the analysis of craniofacial asymmetry

Xiling Jiang[1], Yin Ding[1], Yanyan Zhang[2], Shizhu Bai[3], Xin Chang[4], Bao Liu[5], Kai Liu[6]

[1]State Key Laboratory of Military Stomatology & National Clinical Research Center for Oral Diseases & Shaanxi Clinical Research Center for Oral Diseases, Department of Orthodontics, School of Stomatology, The Fourth Military Medical University, Xi'an 710032, Shaanxi, PR China; [2]Department of Image, Tongliao City Hospital, Tongliao 028000, Inner Mongolia, PR China; [3]State Key Laboratory of Military Stomatology & National Clinical Research Center for Oral Diseases & Shaanxi Key Laboratory of Oral Diseases, Department of Prosthodontics, School of Stomatology, The Fourth Military Medical University, Xi'an 710032, Shaanxi, PR China; [4]Department of Stomatology, The Second Hospital of Dalian Medical University, Dalian 116027, Liaoning, PR China; [5]Department of Image, Fourth Military Medical University's Xi Jing Hospital, Xi'an 710032, Shaanxi, PR China; [6]College of Animal Science and Technology, Inner Mongolia University for The Nationalities, Tongliao 028000, Inner Mongolia, PR China

Received June 12, 2017; Accepted November 2, 2017; Epub December 15, 2017; Published December 30, 2017

Abstract: The purpose of this study was to determine the relationship between the anterior cerebral falx plane and anatomical landmarks on the craniofacial midline. In addition, the anterior cerebral falx was evaluated for use as a median sagittal reference plane. Patients attending the Tong Liao City Hospital emergency center were included in this study as the control group (no visible craniofacial asymmetry). Subjects being treated at the Fourth Military Medical University in the Department of Orthodontics were placed into an asymmetrical group (craniofacial asymmetry). Each group included 50 subjects. In the computed tomography (CT) images, the anterior cerebral falx plane was manually extracted, and anatomical landmarks were selected on the craniofacial midline. The vertical distances from anatomical landmarks to the anterior cerebral falx plane were measured. The relationships between the anterior cerebral falx plane and anatomical landmarks on the craniofacial midline in the control and asymmetrical groups were verified, while the median sagittal cerebral falx plane and the median sagittal plane constructed using the three-point method were compared. In the control group, the anterior cerebral falx almost passed the craniofacial midline. In the asymmetrical group, the craniofacial asymmetry was mainly focused on the lower jaw, and the deviation of the facial midline from the falx was aggravated gradually from top to bottom. The anterior cerebral falx plane was a median sagittal craniofacial plane confirmed by morphology and evolutionary developmental biology. The anterior cerebral falx can be considered a sensitive and stable reference plane for studying craniofacial asymmetry.

Keywords: Cerebral falx, craniofacial midline, craniofacial asymmetry

Introduction

The symmetrical growth of craniofacial structures is very important to patient aesthetics [1]. The human face develops with bilateral symmetry, resulting in two identical sides [2]. Ideally, the right and left halves should have identical structures [1]. Asymmetry of the human craniofacial skeleton is a common finding in orthodontic patients and non-patients. The degree of asymmetry varies from gross discrepancies that interfere with the physiological function and aesthetics, to minor asymmetry that may remain unnoticed by the individual [3]. There are a number of etiological factors (genetic and environmental) associated with craniofacial asymmetry [4, 5], and asymmetry may be congenital (clefts, microsomia), developmental (condylar hyperactivity) or acquired (trauma, skeletal tumors) [6].

To diagnose craniofacial asymmetry, it is essential to determine the median sagittal reference plane. A number of anatomical landmarks of the craniofacial midline such as the nasion (N), anterior nasal spine (ANS), posterior nasal spine (PNS), sella (S), basion (Ba), crista galli (Cr), and opisthion (Op) are commonly used to construct the median sagittal plane [7-10]. With another method, the median sagittal plane can

Table 1. Anatomical landmarks on the craniofacial midline

Anterior cranial base	Cr	The most superior edge of the crista galli
Medial cranial base	Cl	Midpoint between the anterior clinoid processes
Posterior cranial base	Op	Midpoint of the posterior arch of the foramen magnum
Upper face	MZF	Midpoint between bilateral uppermost points of zygomaticofrontal suture
	N	Nasofrontal suture at the midline
Middle face	ANS	The most anterior midpoint of the anterior nasal spine of the maxilla
	PNS	The most posterior midpoint of the posterior nasal spine of the palatine bone
	UI	Contact point of the two central upper incisor teeth
Lower face	LI	Contact point of the two central lower incisor teeth
	Me	The most inferior point in the mandibular symphysis

first be defined using the horizontal plane as a reference landmark [11, 12]. Alternatively, Gateno [13] recommended to construct an extracranial reference system irrelevant to the intracranial anatomical structures using the natural head position. Damstra [14] developed the craniofacial symmetric plane (morphometric median sagittal plane) using the morphometric method. Although many methods have been used to determine the median sagittal plane, each method has certain limitations and experts are currently lacking a widely accepted method to define the median sagittal plane.

Numerous studies have revealed that the brain, cranium, and face have covariant or integrated developmental systems [15-23]. The forebrain, anterior cranial base, and mid-upper facial midline are regulated by the same signaling factors, and are therefore highly consistent [24-27]. The prechordal plate produces molecular signals such as sonic hedgehog (SHH) that determines the median line for the face, patterns the forebrain into two separate hemispheres, and separates the eye fields into two areas [28]. The cerebral falx (sickle-like tough fibrous dural fold) is another important landmark that projects downward from the midline of the cranial vault into the sagittal fissure of cerebrum [29]. The cerebral falx is a midsagittal plane of the brain which separates the brain into two similar halves, or hemispheres. Therefore, it can replace the average distance between the inner tables of the skull as a gold standard midline reference during computed tomography (CT) assessment of brain midline shift [30]. However, the cerebral falx adjacent to the occiput (posterior) has a different embryonic origin [31] and deviates from the midline [32]. We have hypothesized that the anterior cerebral falx plane can be a reliable median sagittal plane for studying craniofacial asymmetry. The aim of this study was to determine the relationship between the anterior cerebral falx plane and the facial midline. In addition, we have compared the correlation between the median sagittal cerebral falx plane and the median sagittal plane constructed using the three-point method.

Materials and methods

Study design

This was a retrospective study, conducted using the radiographic data of patients attending the Department of Orthodontics at the Fourth Military Medical University, Xi'an, Shaanxi Province of China. This study was reviewed and approved by the Ethics Committee at the Tong Liao City hospital. Informed consent was waived by the committee due to the retrospective nature of the study. Patients who attended the hospital between March 2013 and January 2016, and were suffering from craniofacial asymmetry, were included. All subjects (n=100) who fulfilled the selection criteria were randomly divided into two groups (n=50 per group; control and asymmetry). The inclusion criteria were: adults (≥ 18 years of age) having complete dentition and centric jaw position, with a scan ranging from the calvaria to the lower edge of the mandible. The exclusion criteria included: craniofacial injuries or bone fractures, diffuse inflammation, brain abnormalities or soft tissue tumors, grossly decayed teeth, crowding more than 3 mm or spacing more than 1 mm, a history of previous orthodontic or orthognathic treatment, and cleft lip/palate patients.

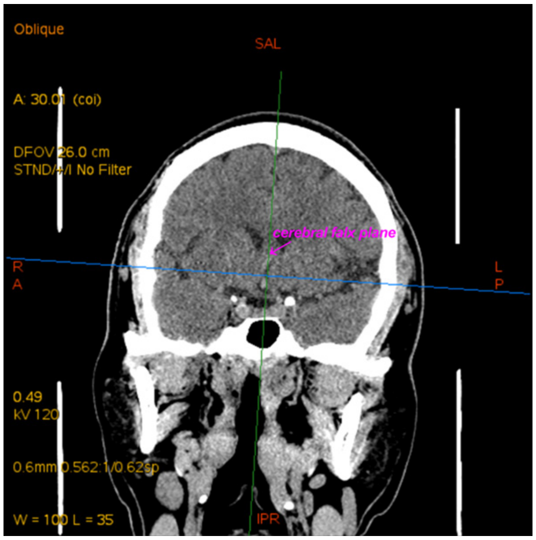

Figure 1. Three dimensional (3D) determination of the cerebral falx plane: Step 1. Performed using GE Advanced Workstation 4.5 VolumeShare 4 platform (Volume Viewer, Volume Rendering). An original 3D coordinate system consists of green, blue, and yellow lines that represent three axes, which are always perpendicular to each other. The green axis was selected to represent the cerebral falx plane. At the coronal position anterior to the hypophyseal foramen, the green axis was made to completely coincide with the cerebral falx. This coincident line was the coronal intersecting line between the location of the green axis plane and the cerebral falx plane, and was used to upright the head (**Figure 1**).

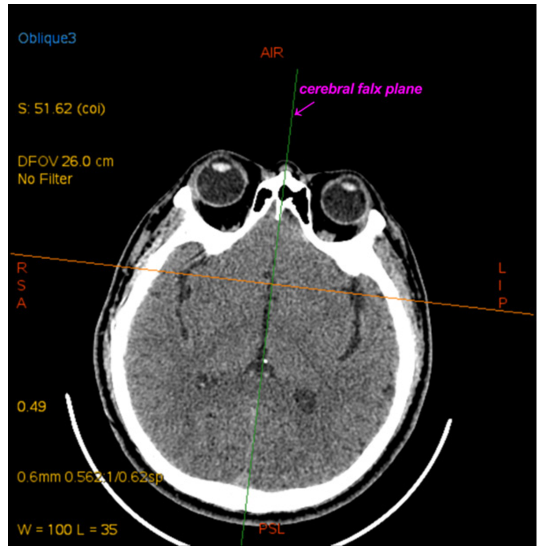

Figure 2. Three dimensional (3D) determination of the cerebral falx plane: Step 2. The green axis was held stationary and the angle between the green line and the cerebral falx was observed from the horizontal position. This angle was the horizontal intersecting angle between the green axis location plane and the cerebral falx location plane, wherein the intersecting point in the 3D point of view was the coincident line as mentioned in **Figure 1**. Taking this intersecting point as the origin, the green axis was rotated to be coincident with the cerebral falx completely. From top to bottom, the green axis is further corrected to maximally coincide with the cerebral falx at all horizontal levels.

CT scans were obtained using a spiral CT scanner (Light Speed PRO, GE Medical Systems, Milwaukee, Wisconsin) with fixed parameters (2.5 mm thickness, slice pitch 3, and a scanning time of 1.0 second). The patient was scanned in a supine position. The gantry had zero inclination, and the scanning matrix was set at 512×512 pixels. After the scanning was complete, digital imaging and communication in medicine (DICOM) images were created in 0.625 mm-thick slices. The acquired two-dimensional (2D) CT DICOM data were then transferred to a computer. The three-dimensional (3D) images were created by using GE Advanced Workstation 4.5 (GE Medical Systems, Buc Cedex, France).

In the asymmetry group, two independent researchers analyzed craniofacial midline anatomical landmarks (**Table 1**) and confirmed the visible craniofacial asymmetry. For example, the deviation of the mandibular symphysis (Me) from the median sagittal plane constructed by Cr, ANS, and Op landmarks (**Table 1**) was greater than 4 mm in the asymmetrical group.

Patients in the control group were selected from the emergency room of the Tong Liao City Hospital Tongliao, Inner Mongolia, China during the period of study. Two independent researchers analyzed the CT data to rule out the presence of any craniofacial asymmetry in the control group. Deviation of the Me from the median sagittal plane constructed by Cr, ANS, and Op, was considered control at less than 2 mm.

Establishment of median sagittal cerebral falx plane

Using an AW VolumeShare 4 platform (Volume Viewer, Volume Rendering), the horizontal, sagittal, and coronal CT data were entered in the 3D coordinate system. As seen in **Figure 1**, one of the axes was selected as the longitudinal axis (such as the green line), which represented a plane in the 3D space. The following proce-

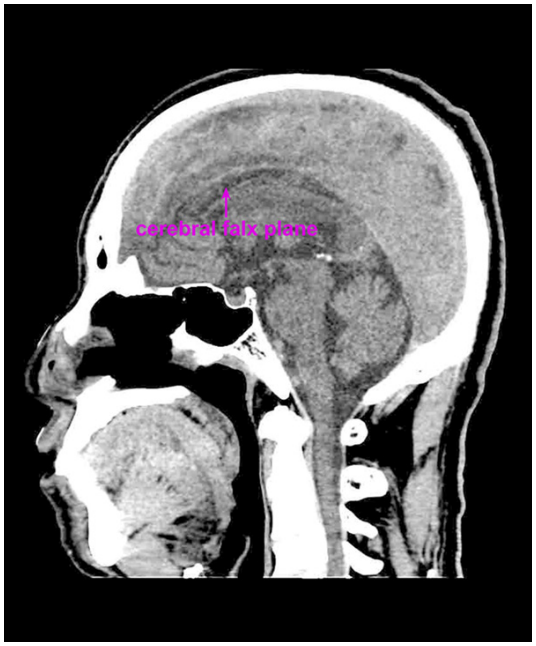

Figure 3. Three dimensional (3D) determination of the cerebral falx plane: Step 3. To further verify the cerebral falx, on the sagittal plane the cerebral falx appears as a translucent membrane, and doesn't contain any brain tissue. The cerebral falx has sickle shape appearance and was observed underneath the septum pellucidum instead of as low-density shadows in the lateral ventricle.

dures were needed to align the chosen plane with the anterior cerebral falx. First, at the coronal position anterior to the hypophyseal foramen, the green line was made to completely coincide with the cerebral falx. In this 3D coordinate system, the blue line automatically changes position in relation to green line movement, while remaining perpendicular to each other. This coincident line was the coronal intersecting line between the green line location plane and the cerebral falx plane, in order to upright the head (**Figure 1**).

The green line was held stationary to observe the angle between this line and the cerebral falx from the horizontal position. This angle was the horizontal intersecting angle between the green line location plane and the cerebral falx location plane, wherein the intersecting point in the 3D point of view was the coincident line, as mentioned in **Figure 1**. Taking this intersecting point as the origin, the green line was rotated to be coincident with the cerebral falx (**Figure 2**).

In the sagittal position, the cerebral falx plane performs fine adjustment. In the sagittal plane,

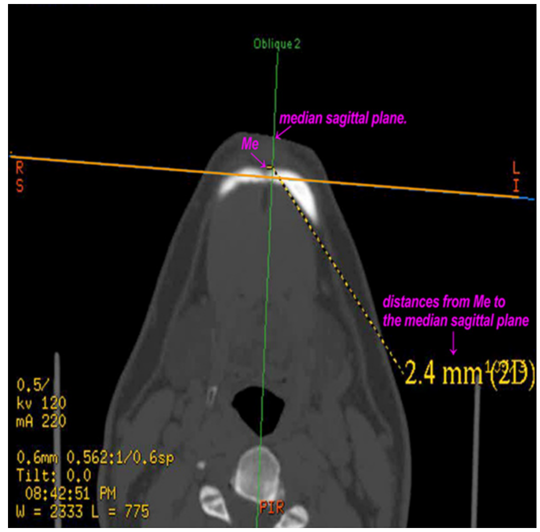

Figure 4. Example of vertical distance measurement from craniofacial midline anatomical landmarks to the median sagittal plane. Me, inferior point of mandibular symphysis.

Table 2. Age and gender distribution in the control and asymmetrical groups

	Control group (n=50)	Asymmetrical group (n=50)
Male	18 (36.0%)	18 (36.0%)
Female	32 (64.0%)	32 (64.0%)
Age (years)	33.5 (18-66)	22 (18-60)
	34.22 ± 11.75	23.96 ± 6.97

the cerebral falx had a sickle-shape appearance and was observed underneath the septum pellucidum instead of as low-density shadows in the lateral ventricle. However, a section of the cerebral falx appeared partially absent. If the posterior cerebral falx appeared deviated, the cerebral falx plane was determined by the anterior cerebral falx. Meanwhile, sagittal sickle images had a high reproducibility (**Figure 3**).

Landmarks (**Table 1**) at the upper, middle, and lower face, as well as at anterior, median, and posterior cranial base midlines were located by rotating the image and viewing it from an optimal angle. Distances between these landmarks and the two median sagittal planes were measured to 0.01 mm in both control and asymmetrical groups. For quantitative analysis, a median sagittal plane constructed using the three-point method based on Cr, ANS, and Op was used to compare the results obtained using the cerebral falx plane (**Figure 4**).

Table 3. Distances between anatomical landmark and the cerebral falx plane in the control and asymmetrical groups

	Control group (n=50)	95% CI	Asymmetrical group (n=50)	95% CI	P
Cr					
Median (min, max)	0 (0, 1.5)		0 (0, 1.6)		0.752
Mean ± SD	0.1 ± 0.36	(-0.01, 0.20)	0.1 ± 0.34	(0.00, 0.20)	
Cl					
Median (min, max)	0.63 (0.05, 3.1)		0.63 (0, 3.25)		0.997
Mean ± SD	0.75 ± 0.57	(0.59, 0.92)	0.92 ± 0.88	(0.67, 1.17)	
Op					
Median (min, max)	1 (0, 3.4)		1.13 (0, 8.8)		0.781
Mean ± SD	1.15 ± 1.08	(0.84, 1.46)	1.41 ± 1.72	(0.93, 1.90)	
MZF					
Median (min, max)	0.55 (0, 1.3)		0.53 (0, 4.35)		0.243
Mean ± SD	0.5 ± 0.32	(0.41, 0.59)	0.73 ± 0.73	(0.52, 0.94)	
N					
Median (min, max)	0 (0, 0.8)		0.5 (0, 2.1)		0.001
Mean ± SD	0.06 ± 0.19	(0.01, 0.12)	0.5 ± 0.53	(0.35, 0.66)	
ANS					
Median (min, max)	0 (0, 1.2)		1.5 (0, 8.8)		0.001
Mean ± SD	0.13 ± 0.29	(0.05, 0.22)	1.87 ± 1.88	(1.33, 2.40)	
PNS					
Median (min, max)	0 (0, 1.7)		1.1 (0, 7.8)		0.001
Mean ± SD	0.23 ± 0.45	(0.10, 0.35)	1.26 ± 1.39	(0.87, 1.66)	
UI					
Median (min, max)	0.6 (0, 2.1)		3.5 (0, 14)		0.001
Mean ± SD	0.64 ± 0.55	(0.48, 0.79)	3.89 ± 3.11	(3.00, 4.77)	
LI					
Median (min, max)	0.8 (0, 3)		5.2 (0, 16.2)		0.001
Mean ± SD	0.93 ± 0.69	(0.74, 1.13)	5.62 ± 3.81	(4.54, 6.70)	
Me					
Median (min, max)	0.75 (0, 2)		11.25 (2.9, 37.4)		0.001
Mean ± SD	0.8 ± 0.72	(0.59, 1.00)	11.95 ± 6.71	(10.04, 13.85)	

$P<0.05$ was considered statistically significant. Distances were measured in mm. Abbreviations: Cr, crista galli (anterior cranial base); Cl, clinoid processes (median cranial base); Op, opisthion (posterior cranial base); MZF, midpoint zygomaticofrontal suture; N, nasion; ANS, anterior nasal spine; PNS, posterior nasal spine; UI, Contact point of the two central upper incisor teeth; LI, Contact point of the two central lower incisor teeth; Me, mandibular symphysis; CI, confidence interval; SD, standard deviation.

Statistical analysis

Statistical analysis was performed using SPSS software (version 22.0, SPSS Inc., Chicago, IL, USA). For quantitative data, both groups were subjected to normality testing using the Shapiro-Wilk method. Normally distributed data were expressed as mean ± standard deviation (SD), and intergroup comparisons were performed using *t*-tests. Data without normal distribution were described as median (range), and were compared using the non-parametric Mann-Whitney U test. In addition, Spearman's method was used to analyze the correlations among various landmarks in both control and asymmetrical groups. Finally, intragroup correlation coefficient (ICC) was used to determine the consistency between the median sagittal plane defined using the cerebral falx, compared to that defined by the three-point method.

Results

The general distribution of gender and age of participants is shown in **Table 2**. There were 18 (36%) male and 32 (64%) female patients in

Table 4. Distances between anatomical landmarks and the reference plane constructed by the three-point method in the control and asymmetrical groups.

	Control group (n=50)	95% CI	Asymmetrical group (n=50)	95% CI	P
Cr					
Median (min, max)	0 (0, 0)		0 (0, 0)		1.000
Mean ± SD	0 ± 0		0 ± 0		
Cl					
Median (min, max)	0.85 (0.1, 3.1)		0.7 (0, 2.7)		0.787
Mean ± SD	0.88 ± 0.63	(0.69, 1.06)	0.94 ± 0.69	(0.73, 1.14)	
Op					
Median (min, max)	0 (0, 0)		0 (0, 0)		1.000
Mean ± SD	0 ± 0		0 ± 0		
MZF					
Median (min, max)	0.45 (0, 2.25)		0.6 (0, 5.05)		0.108
Mean ± SD	0.57 ± 0.51	(0.42, 0.73)	0.81 ± 0.86	(0.57, 1.05)	
N					
Median (min, max)	0 (0, 1.4)		0.75 (0, 2.4)		0.001
Mean ± SD	0.21 ± 0.39	(0.09, 0.33)	0.73 ± 0.7	(0.53, 0.94)	
ANS					
Median (min, max)	0 (0, 0)		0 (0, 0)		1.000
Mean ± SD	0 ± 0		0 ± 0		
PNS					
Median (min, max)	0 (0, 1.5)		0 (0, 3.1)		0.002
Mean ± SD	0.13 ± 0.36	(0.02, 0.24)	0.56 ± 0.79	(0.33, 0.79)	
UI					
Median (min, max)	0.6 (0, 1.6)		1.5 (0, 6)		0.001
Mean ± SD	0.59 ± 0.52	(0.43, 0.74)	1.77 ± 1.38	(1.36, 2.17)	
LI					
Median (min, max)	0.9 (0, 2.4)		3 (0, 9.9)		0.001
Mean ± SD	0.88 ± 0.64	(0.69, 1.08)	3.53 ± 2.44	(2.82, 4.25)	
Me					
Median (min, max)	0.9 (0, 2)		10.1 (1.7, 25.8)		0.001
Mean ± SD	0.87 ± 0.69	(0.67, 1.08)	9.67 ± 5.56	(8.03, 11.30)	

P<0.05 was considered statistically significant. Distances were measured in mm. Abbreviations: Cr, crista galli (anterior cranial base); Cl, clinoid processes (median cranial base); Op, opisthion (posterior cranial base); MZF, midpoint zygomaticofrontal suture; N, nasion; ANS, anterior nasal spine; PNS, posterior nasal spine; UI, Contact point of the two central upper incisor teeth; LI, Contact point of the two central lower incisor teeth; Me, mandibular symphysis; CI, confidence interval; SD, standard deviation.

each group. In the control group, the mean distances between landmarks and the cerebral falx plane were less than 1 mm (**Table 3**). The only exception greater than 1 mm was the mean distance between Op and the cerebral falx plane. In the asymmetry group, the mean distances from the Cr, Cl, MZF, and N to the cerebral falx plane were less than 1 mm, while the mean distances from the ANS, PNS, UI, LI to the cerebral falx plane were greater than 1 mm. Furthermore, the mean distances were gradually increased from the upper to lower face. Points below N (including N, ANS, PNS, UI, LI and Me) were significantly different between the control and asymmetrical groups. In addition, although the mean distance from Op to the cerebral falx plane was greater than 1 mm in both groups, the difference between these two groups was not statistically significant (**Table 3**).

Similar to the results obtained using the cerebral falx plane as the reference, the landmarks N, PNS, UI, LI and Me showed statistically sig-

Table 5. Correlation between anatomical landmarks in the control group using the distance to the cerebral falx plane as the reference

	Cr	Cl	Op	MZF	N	ANS	PNS	UI	LI	Me
Cr	1.00	-0.148	-0.354*	.003	0.145	0.033	-0.025	0.222	0.304*	0.095
Cl		1.000	0.105	-0.188	-0.113	-0.076	0.055	-0.009	-0.285*	-0.188
Op			1.000	0.233	-0.037	0.354*	0.244	-0.118	-0.049	0.008
MZF				1.000	0.037	0.168	0.046	0.032	0.211	0.250
N					1.000	0.316*	0.232	0.091	0.073	0.216
ANS						1.000	0.111	0.114	0.172	0.048
PNS							1.000	-0.096	0.156	0.242
UI								1.000	0.463**	0.276
LI									1.000	0.437**
Me										1.000

*P<0.05, **P<0.01. Abbreviations: Cr, crista galli (anterior cranial base); Cl, clinoid processes (median cranial base); Op, opisthion (posterior cranial base); MZF, midpoint zygomaticofrontal suture; N, nasion; ANS, anterior nasal spine; PNS, posterior nasal spine; UI, Contact point of the two central upper incisor teeth; LI, Contact point of the two central lower incisor teeth; Me, mandibular symphysis.

Table 6. Correlation between anatomical landmarks in the asymmetrical group by using the distance to the cerebral falx plane as the reference

	Cr	Cl	Op	MZF	N	ANS	PNS	UI	LI	Me
Cr	1.000	0.200	0.293*	0.175	0.201	0.256	00.215	0.010	-00.158	0.088
Cl		1.000	0.193	0.263	-0.046	0.014	0.025	0.220	0.301*	0.150
Op			1.000	0.207	0.054	0.136	0.169	0.085	0.088	0.007
MZF				1.000	0.251	0.186	0.234	0.021	0.085	0.126
N					1.000	0.362**	0.430**	0.022	0.085	0.065
ANS						1.000	0.674**	0.678**	0.534**	0.475**
PNS							1.000	0.507**	0.466**	0.359*
UI								1.000	0.738**	0.597**
LI									1.000	0.736**
Me										1.000

*P<0.05, **P<0.01. Abbreviations: Cr, crista galli (anterior cranial base); Cl, clinoid processes (median cranial base); Op, opisthion (posterior cranial base); MZF, midpoint zygomaticofrontal suture; N, nasion; ANS, anterior nasal spine; PNS, posterior nasal spine; UI, Contact point of the two central upper incisor teeth; LI, Contact point of the two central lower incisor teeth; Me, mandibular symphysis.

nificant differences between the control group and asymmetrical group when using the medial sagittal plane (determined by three-point method) as the reference (**Table 4**). In addition, the mean distances from PNS, UI, LI and Me to the reference plane determined by the three-point method were smaller than those to the cerebral falx reference plane. Designating ANS as zero in the three-point method concealed craniofacial asymmetry below ANS.

From **Table 6**, in the asymmetrical group, ANS, UI, LI were correlated with Me strongly and directly. Therefore, their deviation from the cerebral falx plane was strongly and directly correlated with Me deviation. These data suggested that most of the functional and inherent craniofacial asymmetry were derived from the lower jaw and transferred to the upper face via asymmetric contraction of muscle modules bilaterally.

When comparing **Table 5** and **Table 6** data, in the control group, the LI was directly correlated only with Me, whereas UI was strongly correlated only with LI. Since LI is on the mandible, the normal range of Me point deviation is strongly correlated with LI, and UI was strongly correlated with LI due to the direct occlusal contact between the upper and lower teeth. However, the normal range deviation of Me from cerebral falx plane is not strong enough to cause midline deviation of the landmarks superior to the mandible.

Table 7. Consistency of results at anatomical landmarks using the median sagittal planes determined by the cerebral falx and the three-point method as references

	ICC	P
CI	0.613	0.000
MZF	0.820	0.000
N	0.685	0.000
PNS	0.481	0.001
UI	0.550	0.000
LI	0.803	0.000
Me	0.920	0.000

Abbreviations: CI, clinoid processes (median cranial base); MZF, midpoint zygomaticofrontal suture; N, nasion; PNS, posterior nasal spine; UI, Contact point of the two central upper incisor teeth; LI, Contact point of the two central lower incisor teeth; Me, mandibular symphysis; ICC, intragroup correlation coefficient.

Consistency between the two methods was represented using intragroup correlation coefficient (ICC) analysis, of which 0.1 referred to absence of consistency and 1 referred to complete consistency (**Table 7**). Generally, a reliability coefficient <0.4 is considered poor consistency, while a reliability coefficient >0.75 is considered good consistency [33].

The median sagittal planes determined using the two methods showed consistency in terms of CI, MZF, N, PNS, UI, LI and Me, with the best consistency observed for MZF, LI and Me (**Table 7**).

Discussion

The current study has determined the relationships between the anterior cerebral falx plane and midline craniofacial anatomical landmarks, and has suggested using the anterior cerebral falx as the median sagittal reference plane for evaluation of craniofacial asymmetry. Patient CT data was retrospectively analyzed and various midline landmarks were identified for the assessment of craniofacial asymmetry. The anterior cerebral falx is an actual, precise, and stable median sagittal plane that is in line with evolutionary development and molecular biology. The cerebral falx serves as a midline barrier that forms due to folding of the dura mater, and divides the human brain into two halves. The cerebral falx can be identified easily in high-resolution CT scans and manifests as a high-density line in the axial position [29].

The current study reported that the majority of craniofacial midline anatomical landmarks including N, ANS, and Me were intersecting points of bilaterally symmetrical structures distinguishable in CT scans. These anatomical landmarks are frequently used to determine the median sagittal plane. In the normal population, the current study reported that the mean distance of the landmarks to the two defined reference planes were less than 1 mm. The only exception was Op, which was greater than 1 mm for both the control and asymmetrical groups. In addition, in the case of unnoticed craniofacial symmetry populations, the brain midline almost passed the craniofacial midline, and the anterior cerebral falx plane remained at the craniofacial center. These findings have indicated that the human craniofacial region is a symmetrical structure with respect to the medial axis of the central nervous system in the normal population.

These findings are consistent with the neuroanatomical aspects in which the falx can replace the average distance between the inner tables of the skull, and is considered a gold standard midline reference for brain midline shift assessment [30]. In addition, these data further verified the opinion that the midlines of the forebrain, anterior skull, and mid-upper face are highly associated in evolutionary development, molecular biology, and clinical medicine [24-28].

The mean distances of landmarks (PNS, UI, LI and Me) to the reference plane determined by the three-point method were smaller than those to the cerebral falx plane. Since the ANS is assigned as zero in the three-point method, this conceals the deviation of the ANS and asymmetry of the mid-face. Therefore, the median sagittal plane determined by the cerebral falx is more precise than the plane determined by the three-point method. In addition, in patients with severe craniofacial asymmetry, the mean distances from the Cr, CI, MZF and N to the cerebral falx plane were less than 1 mm, which indicated that the cerebral falx plane was stable in such patients while still passing the midline of the anterior skull base and upper face. The craniofacial asymmetry is usually exaggerated gradually from top to bottom. This phenomenon can be interpreted by the modular organization of human head, and thus pro-

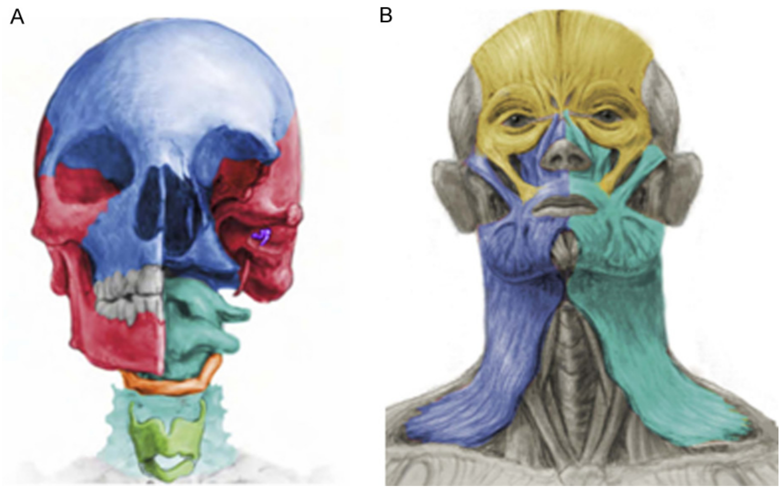

Figure 5. Esteve-Altava Skeleton and muscle modules of human head based on anatomical networks [45]. A. Red, the cranial complex; blue, the facial complex; green, the thyroid complex; yellow, the thoracic complex; cyan, the cervical complex; light and dark purple, the ossicle complexes; and orange, the hyoid one-bone module. B. Modules of the head musculature identified using AnNA. In yellow, the ocular/upper face complex; in light and dark blue, the orofacial complexes; and in grey, the 21 smaller blocks of inter-connected muscles. In the absence of bones, most muscles are totally disconnected from the three major muscle modules (in white). Strength of modularity (Q-value) 0.8323. This figure was drawn by Christopher Smith.

vides new evidence for the New Head Hypothesis (NHH) [34]. In patients with craniofacial asymmetry, the distance between midline landmarks from the upper to lower face and the anterior cerebral falx plane have been reported to increase gradually and consistently according to results obtained by other reference planes [35-41]. In addition, the mean distances from CI, MZF and N to the two reference planes were less than 1 mm in the asymmetry group. In terms of median sagittal planes determined by the cerebral falx and three-point methods, the landmarks superior to N were not different between the control and asymmetrical groups, which was consistent with the results reported previously [39]. A similar pattern of asymmetry in the upper third of the face has been reported in patients with no asymmetry and patients with varying degrees of asymmetry [39]. Although the mean distance between the Op and the cerebral falx plane was larger than 1 mm in the control and asymmetry groups, the difference between these two groups was not significant, indicating that the skull base was still principally symmetric.

These common onsets of craniofacial asymmetry can be interpreted by modular organization of human head that provides new evidence for the NHH and mosaic evolution. Modular development is the key mechanism to improve bioavailability and stability of living organisms. Along the antero-posterior axis (cephalocaudal axis), cranial skeletons are derived from different germ layers. The anterior aspect of the skull develops from neural crest cells (ectoderm). The posterior aspect of skull, the boundary of the two halves in the sagittal suture at the dorsal side, and near the hypophyseal foramen at the ventral side are derived from the mesoderm [20, 42]. The occipital bone exist in the form of an enlarged spine that supports the entire brain [34, 42]. Additionally, the anterior and posterior skull components are regulated by different genes [43]. According to the NHH proposed by Gans and Northcutt, the rostral head of vertebrates is a neomorphic unit. The "new head" derived from neural crest, allows a shift from filter feeding to active predation. The neural crest-mesoderm boundary should correlate with the rostral-most tip of the notochord, thereby creating a coincident boundary with the prechordal-chordal boundary in the cranium [34]. The trigeminal crest cells give rise to the pre-mandibular and mandibular components of the cranium, and the former corresponds to the prechordal cranium [44]. The anterior cranium (prechordal cranium) with the mid-upper face (pre-mandibular components) and the posterior cranium with the lower jaw, respectively form two craniofacial skeletal modules (**Figure 5**). The upper face above the eyebrow forms a single musculoskeletal module [45]. In this study, the distance between midline landmarks from upper to lower faces and the anterior cerebral falx plane were gradually increased in patients with craniofacial asymmetry, and the ANS, UI, LI were strongly correlated with Me directly. This is suggestive that most of the functional and inherent craniofacial asymmetry are derived from the lower jaw and are transferred to the upper face via asymmetrical contraction of muscle modules bilaterally. Alternatively, the bilateral upper-lower jaw muscle modules may experience functional asymmetric contractions leading to asymmetry of the lower jaw, prior to asymmetry of the upper face. The anterior cranium and mid-upper facial module is relatively stable, especially the upper third of the face. These findings further confirm the conclusions made in a human head anatomical network analysis, which described the upper face as a single module of nerve, skeleton and muscle, and therefore it has the best symmetry [45, 46]. Furthermore, there was minor deviation of Op and Me from the cerebral falx in the control group. The Me was more prone to deviation in the asymmetrical group, suggesting that the midline alignment between the anterior and posterior skulls, as well as the upper and lower jaws, are poorly regulated compared to within each module.

There are a number of limitations in this study. First, the craniofacial data were obtained from spinal CT scans. Using CT scans for diagnostic purpose involves a higher radiation dose compared to conventional radiography. Considering the ethical issues and risks involved in exposing healthy individuals to high amount of radiation solely for research purposes, this study was conducted using the retrospective CT data available from routine investigations. Second, manual positioning of the cerebral falx is cumbersome. It will be necessary to develop a method to automatically extract the cerebral falx plane using computer software. Third, although large-field cone-beam CT is capable of whole-brain scanning, cone-beam CT imaging of soft tissues is comparatively less clear. However, this method of determining the median sagittal plane based on the head symmetry axis is a novel idea for 3D analysis of craniofacial asymmetry. In addition, the authors for the first time used a modularization viewpoint to explain the aggravating asymmetry from the upper to lower face. The subjects in this study had craniofacial asymmetry and were not classified according to malocclusion.

In conclusion, the anterior cerebral falx plane is a physical median sagittal cerebral-craniofacial plane that has been confirmed by evolutionary development and morphology. It can be considered a sensitive reference plane for the assessment and diagnosis of craniofacial asymmetry. The anterior cerebral falx plane is also relatively stable in patients with severe craniofacial asymmetry.

Acknowledgements

This study was supported by the Natural Science Foundation of Inner Mongolia (No. 2015-MS0855).

Disclosure of conflict of interest

None.

Address correspondence to: Yin Ding, State Key Laboratory of Military Stomatology & National Clinical Research Center for Oral Diseases & Shaanxi Clinical Research Center for Oral Diseases, Department of Orthodontics, School of Stomatology, The Fourth Military Medical University, Xi'an 710032, Shaanxi, PR China. Tel: +86-15848956968; Fax: +86-475-8619108; E-mail: 2274370119@qq.com

References

[1] Orthodontist TA. An assessment of asymmetry in the normal craniofacial complex. Angle Orthodontist 1978; 48: 141-148.
[2] Lindauer SJ. Asymmetries: diagnosis and treatment. Semin Orthod 1998; 4: 133.
[3] Orthodontist TA. Craniofacial asymmetry in development: an anatomical study. Angle Orthodontist 2003; 73: 381-385.
[4] Costa RL Jr. Asymmetry of the mandibular condyle in Haida Indians. Am J Phys Anthropol 1986; 70: 119-123.
[5] Melnik AK. A cephalometric study of mandibular asymmetry in a longitudinally followed sample of growing children. Am J Orthod Dentofacial Orthop 1992; 101: 355-366.
[6] Patel PK, Jacobson R and Zhao L. Craniofacial asymmetry: causes and management: principles, planning and practice. 2016.
[7] Alhadidi A, Cevidanes L, Mol A, Ludlow J and Styner M. Comparison of two methods for quantitative assessment of mandibular asymmetry using cone beam computed tomography image volumes. Dento Maxillo Facial Radiology 2011; 40: 351-357.
[8] Lee H, Bayome M, Kim SH, Kim KB, Behrents RG and Kook YA. Mandibular dimensions of subjects with asymmetric skeletal class III malocclusion and normal occlusion compared with cone-beam computed tomography. Am J Orthod Dentofacial Orthop 2012; 142: 179-85.

[9] Sievers MM, Larson BE, Gaillard PR and Wey A. Asymmetry assessment using cone beam CT. A class I and class II patient comparison. Angle Orthodontist 2012; 82: 410.
[10] Kheir NA and Kau CH. Measuring mandibular asymmetry in class I normal subjects using 3D novel coordinate system. Ann Maxillofac Surg 2014; 4: 34-38.
[11] Nur RB, DG Ç and Arun T. Evaluation of facial hard and soft tissue asymmetry using cone-beam computed tomography. Am J Orthod Dentofacial Orthop 2016; 149: 225-237.
[12] Shin SM, Kim YM, Kim NR, Choi YS, Park SB and Kim YI. Statistical shape analysis-based determination of optimal midsagittal reference plane for evaluation of facial asymmetry. Am J Orthod Dentofacial Orthop 2016; 150: 252-60.
[13] Gateno J, Xia JJ and Teichgraeber JF. New 3-dimensional cephalometric analysis for orthognathic surgery. J Oral Maxillofac Surg 2011; 69: 606-22.
[14] Damstra J, Fourie Z, Wit MD and Ren Y. A three-dimensional comparison of a morphometric and conventional cephalometric midsagittal planes for craniofacial asymmetry. Clinical Oral Investigations 2012; 16: 285-294.
[15] Richtsmeier JT, Aldridge K, Deleon VB, Panchal J, Kane AA, Marsh JL and Yan P. Phenotypic integration of neurocranium and brain. J Exp Zool B Mol Dev Evol 2006; 306: 360-378.
[16] Nie X. Cranial base in craniofacial development: developmental features, influence on facial growth, anomaly, and molecular basis. Acta Odontol Scand 2005; 63: 127.
[17] Marcucio RS, Young NM, Hu D and Hallgrimsson B. Mechanisms that underlie co-variation of the brain and face. Genesis 2011; 49: 177.
[18] Aoto K and Trainor PA. Co-ordinated brain and craniofacial development depend upon patched1/XIAP regulation of cell survival. Hum Mol Genet 2015; 24: 698-713.
[19] Parsons TE, Schmidt EJ, Boughner JC, Jamniczky HA, Marcucio RS and Hallgrímsson B. Epigenetic integration of the developing brain and face. Dev Dyn 2011; 240: 2233-44.
[20] Richtsmeier JT and Flaherty K. Hand in glove: brain and skull in development and dysmorphogenesis. Acta Neuropathol 2013; 125: 469-89.
[21] Aldridge K, Kane AA, Marsh JL, Yan P, Govier D and Richtsmeier JT. Relationship of brain and skull in pre- and postoperative sagittal synostosis. J Anat 2005; 206: 373-385.
[22] Tubbs RS, Bosmia AN and Cohengadol AA. The human calvaria: a review of embryology, anatomy, pathology, and molecular development. Childs Nerv Syst 2012; 28: 23-31.
[23] Ferros I, Mora MJ, Obeso IF, Jimenez P and Martinezinsua A. The nasomaxillary complex and the cranial base in artificial cranial deformation: relationships from a geometric morphometric study. Eur J Orthod 2015; 37: 403-11.
[24] Fong KS, Adachi DA, Chang SB and Lozanoff S. Midline craniofacial malformations with a lipomatous cephalocele are associated with insufficient closure of the neural tube in the tuft mouse. Birth Defects Res A Clin Mol Teratol 2014; 100: 598-607.
[25] Petryk A, Graf D and Marcucio R. Holoprosencephaly: signaling interactions between the brain and the face, the environment and the genes, and the phenotypic variability in animal models and humans. Wiley Interdiscip Rev Dev Biol 2015; 4: 17-32.
[26] Fong KS, Cooper TB, Drumhiller WC, Somponpun SJ, Yang S, Ernst T, Chang L, Lozanoff S. Craniofacial features resembling frontonasal dysplasia with a tubulonodular interhemispheric lipoma in the adult 3H1 tuft mouse. Birth Defects Res A Clin Mol Teratol 2012; 94: 102-113.
[27] Brugmann SA, Allen NC, James AW, Mekonnen Z, Madan E and Helms JA. A primary cilia-dependent etiology for midline facial disorders. Hum Mol Genet 2010; 19: 1577-1592.
[28] Gondrélewis MC, Gboluaje T, Reid SN, Lin S, Wang P, Green W, Diogo R, Fidélialambert MN and Herman MM. The human brain and face: mechanisms of cranial, neurological and facial development revealed through malformations of holoprosencephaly, cyclopia and aberrations in chromosome 18. J Anat 2015; 227: 255-67.
[29] Osborn AG, Anderson RE and Wing SD. The false falx sign. Radiology 1980; 134: 421-425.
[30] Caricato A. What is the gold standard method for midline structures shift assessment using computed tomography? Crit Care Med 2012; 40: 3332-3333.
[31] Shigeru K and Thomas S. Head segmentation in vertebrates. Integr Comp Biol 2008; 48: 604-610.
[32] Glicksohn J and Myslobodsky MS. The representation of patterns of structural brain asymmetry in normal individuals. Neuropsychologia 1993; 31: 145-159.
[33] Cicchetti DV. Guidelines, criteria, and rules of thumb for evaluating normed and standardized assessment instruments in psychology. Psychological Assessment 1994; 6: 284-290.
[34] Northcutt RG and Gans C. The genesis of neural crest and epidermal placodes: a reinterpretation of vertebrate origins. Q Rev Biol 1983; 58: 1-28.
[35] Damstra J, Fourie Z and Ren Y. Evaluation and comparison of postero-anterior cephalograms and cone-beam computed tomography images

for the detection of mandibular asymmetry. Eur J Orthod 2013; 35: 45-50.
[36] Kim EJ, Palomo JM, Kim SS, Lim HJ, Lee KM and Hwang HS. Maxillofacial characteristics affecting chin deviation between mandibular retrusion and prognathism patients. Angle Orthod 2011; 81: 988-993.
[37] Proffit WR, Phillips C and Th DC. Who seeks surgical-orthodontic treatment? Int J Adult Orthodon Orthognath Surg 1990; 5: 153-60.
[38] Severt TR and Proffit WR. The prevalence of facial asymmetry in the dentofacial deformities population at the university of North Carolina. Int J Adult Orthodon Orthognath Surg 1997; 12: 171-6.
[39] Park JU, Kook YA and Kim Y. Assessment of asymmetry in a normal occlusion sample and asymmetric patients with three-dimensional cone beam computed tomography a study for: a transverse reference plane. Angle Orthod 2012; 82: 860-7.
[40] Baek SH, Cho IS, Chang YI and Kim MJ. Skeletodental factors affecting chin point deviation in female patients with class III malocclusion and facial asymmetry: a three-dimensional analysis using computed tomography. Oral Surg Oral Med Oral Pathol Oral Radiol Endod 2007; 104: 628-639.
[41] Haraguchi S, Takada K and Yasuda Y. Facial asymmetry in subjects with skeletal class III deformity. Angle Orthodontist 2002; 72: 28-35.
[42] Berry C. Ahead of the head. QJM 2002; 95: 415-416.
[43] Neil MC, Alfire S, Bertrand JY and Eberhart JK. An Fgf-Shh signaling hierarchy regulates early specification of the zebrafish skull. Developmental Biology 2016; 415: 261.
[44] Kuratani S. Cephalic neural crest cells and the evolution of craniofacial structures in vertebrates: morphological and embryological significance of the premandibular-mandibular boundary. Zoology 2005; 108: 13-25.
[45] Estevealtava B, Diogo R, Smith C, Boughner JC and Rasskingutman D. Anatomical networks reveal the musculoskeletal modularity of the human head. Sci Rep 2015; 5: 8298.
[46] Estevealtava B, Boughner JC, Rui D, Villmoare BA and Rasskingutman D. Anatomical network analysis shows decoupling of modular lability and complexity in the evolution of the primate skull. PLoS One 2015; 10: e0127653.